

Attenuated Accumulation of Novel Fluorine (^{19}F)-Labeled Bile Acid Analogues in Gallbladders of Fibroblast Growth Factor-15 (FGF15)-Deficient Mice

Melissa Metry, Jessica Felton, Kunrong Cheng, Su Xu, Yong Ai, Fengtian Xue, Jean-Pierre Raufman, and James E Polli

Mol. Pharmaceutics, **Just Accepted Manuscript** • DOI: 10.1021/acs.molpharmaceut.8b00454 • Publication Date (Web): 24 Sep 2018

Downloaded from <http://pubs.acs.org> on September 26, 2018

Just Accepted

“Just Accepted” manuscripts have been peer-reviewed and accepted for publication. They are posted online prior to technical editing, formatting for publication and author proofing. The American Chemical Society provides “Just Accepted” as a service to the research community to expedite the dissemination of scientific material as soon as possible after acceptance. “Just Accepted” manuscripts appear in full in PDF format accompanied by an HTML abstract. “Just Accepted” manuscripts have been fully peer reviewed, but should not be considered the official version of record. They are citable by the Digital Object Identifier (DOI®). “Just Accepted” is an optional service offered to authors. Therefore, the “Just Accepted” Web site may not include all articles that will be published in the journal. After a manuscript is technically edited and formatted, it will be removed from the “Just Accepted” Web site and published as an ASAP article. Note that technical editing may introduce minor changes to the manuscript text and/or graphics which could affect content, and all legal disclaimers and ethical guidelines that apply to the journal pertain. ACS cannot be held responsible for errors or consequences arising from the use of information contained in these “Just Accepted” manuscripts.



1
2
3
4 **Attenuated Accumulation of Novel Fluorine (¹⁹F)-Labeled Bile Acid Analogues in**
5 **Gallbladders of Fibroblast Growth Factor-15 (FGF15)-Deficient Mice**
6
7
8
9

10 Melissa Metry[†], Jessica Felton[‡], Kunrong Cheng[§], Su Xu^{||}, Yong Ai[†], Fengtian Xue[†], Jean-Pierre
11 Raufman[§], and James E. Polli[†] *
12
13
14
15

16 [†] Department of Pharmaceutical Sciences, University of Maryland School of Pharmacy,
17 Baltimore, Maryland, 21201, United States
18
19

20 [‡] Department of Surgery, University of Maryland School of Medicine, Baltimore, Maryland,
21 21201, United States
22
23

24 [§] VA Maryland Healthcare System, and the Department of Medicine, Division of
25 Gastroenterology & Hepatology, and the Marlene and Stewart Greenebaum Comprehensive
26 Cancer Center, University of Maryland School of Medicine, Baltimore, Maryland, 21201, United
27 States
28
29
30

31 ^{||} Department of Diagnostic Radiology and Nuclear Medicine, University of Maryland School of
32 Medicine, Baltimore, Maryland, 21201, United States
33
34
35
36

37 **KEYWORDS:** Bile acid synthesis, fluorine MRI, enterohepatic circulation, FGF15/19, bile acid
38 diarrhea, imaging methods
39
40
41
42

43 ***Address correspondence to:** James E. Polli, Ph.D.
44
45 20 Penn Street, N623
46
47 Baltimore, MD 21201
48
49 Tel: 410-706-8292;
50
51 Fax: 410-706-5017;
52
53 Email: jpolli@rx.umaryland.edu
54
55
56
57
58
59
60

ABSTRACT

Our work has focused on defining the utility of fluorine (^{19}F)-labeled bile acid analogues and magnetic resonance imaging (MRI) to identify altered bile acid transport *in vivo*. In the current study, we explored the ability of this approach to differentiate fibroblast growth factor-15 (FGF15)-deficient from wild-type (WT) mice, a potential diagnostic test for bile acid diarrhea, a commonly misdiagnosed disorder. FGF15 is the murine homologue of human FGF19, an intestinal hormone whose deficiency is an underappreciated cause of bile acid diarrhea. In a pilot and three subsequent pharmacokinetic studies, we treated mice with two ^{19}F -labeled bile acid analogues, CA-lys-TFA and CA-sar-TFMA. After oral dosing, we quantified ^{19}F -labeled bile acid analogue levels in the gallbladder, liver, small and large intestine, and plasma using liquid chromatography mass spectrometry (LC-MS/MS). Both ^{19}F -bile acid analogues concentrated in the gallbladders of FGF15-deficient and WT mice, attaining peak concentrations at approximately 8.5 h after oral dosing. However, analogue levels in gallbladders of FGF15-deficient mice were several-fold less compared to those in WT mice. Live-animal ^{19}F -MRI provided agreement with our LC-MS/MS-based measures; we detected robust CA-lys-TFA ^{19}F signals in gallbladders of WT mice, but no signals in FGF15-deficient mice. Our finding that ^{19}F -MRI differentiates FGF15-deficient from WT mice provides additional proof-of-concept for the development of ^{19}F -bile acid analogues and ^{19}F MRI as a clinical test to diagnose bile acid diarrhea due to FGF19 deficiency and other disorders.

INTRODUCTION

The past 20 years have witnessed a great expansion in our understanding of the role bile acids play in both normal physiology and disease, as well as the complex processes that maintain bile acid homeostasis.¹ Despite these advances, there remains a paucity of tools to examine bile acid transport *in vivo*. To address this limitation, we investigated the potential of using bile acid analogues labeled with naturally occurring fluorine, ¹⁹F, and *in vivo* magnetic resonance imaging (MRI) to visualize bile acids in anatomical compartments, primarily the gallbladder.²⁻⁴ The work described herein focuses on the potential utility of ¹⁹F-bile acid MRI to diagnose bile acid diarrhea, a condition frequently misdiagnosed as diarrhea-predominant irritable bowel syndrome (IBS-D).⁵

In humans, a gut hormone, fibroblast growth factor-19 (FGF19), governs intestinal feedback regulation of hepatic bile acid synthesis. FGF15 is the murine homologue of FGF19; the designation FGF19/15 refers to processes common to both the human and murine hormones. Bile acids actively absorbed by ileal enterocytes via the apical sodium-dependent bile acid transporter (ASBT, encoded by *SLC10A2*), bind and activate the nuclear farnesoid X receptor (FXR) which, amongst many actions, regulates the production and release of FGF19/15. FGF19/15 circulates to the liver where its interaction with the FGF receptor-4 complex on hepatocytes results in inhibition of hepatocyte 7-alpha-hydroxylase (*CYP7A1*), the rate-limiting enzyme that catalyzes cholesterol hydrolysis and the formation of primary bile acids.

In FGF19/15 deficiency, the absence of feedback regulation of bile acid synthesis results in their excess production, reduced gallbladder filling, and increased levels of bile acids in the distal small intestinal that may overwhelm ASBT transport capacity, thereby increasing bile acid spillage into the colon. Increased fecal bile acid levels in the colon are associated with several harmful effects, including inflammation, altered water and electrolyte secretion, and stimulated motility that may result in diarrhea. Estimates suggest as many as one-third of individuals diagnosed with IBS-D, a common disorder, actually have bile acid diarrhea due to FGF19 deficiency.⁵

For more than 30 years, the most common approach available to diagnose bile acid diarrhea in Europe and Canada has been ⁷⁵Selenium homotaurocholic acid retention testing

1
2
3 (SeHCAT). Although relatively easy to perform, this test requires ingestion of a radiolabeled
4 compound, a nuclear medicine laboratory, and is neither FDA-approved nor available for use in
5 the United States.⁶ Another method, direct measurement of fecal bile acids, is expensive,
6 unavailable in most hospitals and clinics, requires a research laboratory, and performed rarely.
7
8 The recently developed plasma 7α -hydroxy-4-cholestene-3-one (C4) assay is less sensitive and
9 specific than SeHCAT testing and is not widely available. Measuring serum FGF19 levels is
10 possible, but requires additional validation before clinical use.⁷ In the United States, the most
11 common approach to diagnosing bile acid diarrhea remains the exclusion of other causes of
12 diarrhea and a therapeutic trial of a bile acid binder such as cholestyramine or colesevalam.
13 Although decreased diarrhea following treatment with these agents is considered indirect
14 evidence of bile acid diarrhea, this approach is non-specific.⁸
15
16
17
18
19
20
21
22

23 The initial concept driving the current line of investigation was to use MRI, a technique
24 that does not expose individuals to ionizing radiation, to ‘see’ the transport of ^{19}F -labeled bile
25 acid analogues that mimic native bile acid transport in both *in vitro* and *in vivo* studies.^{2-4,9} We
26 chose to image the gallbladder, an organ that concentrates bile acids into the millimolar range,
27 orders of magnitude greater than bile acid concentrations observed in any other organ. In mice
28 gavaged with these fluorinated bile acid probes, we consistently detected a strong ^{19}F -MRI signal
29 in gallbladders of wild-type (WT) mice; ^{19}F -MRI signals were not detected in gallbladders of
30 ASBT-deficient mice.^{2,3} With regard to the present work, we reasoned FGF15-deficient mice
31 would also have a diminished ^{19}F -MRI signal in the gallbladder. We anticipated over-production
32 of native bile acids and their spillage into the gut would dilute ^{19}F -labeled bile acid analogues
33 and increase competition for transport by ASBT. These factors were likely to reduce intestinal
34 uptake, enterohepatic circulation, and gallbladder accumulation of ^{19}F -labeled bile acid probes.
35
36
37
38
39
40
41
42
43

44 In the present study, we investigated the potential utility of ^{19}F -labeled bile acids as tools
45 to diagnose bile acid diarrhea resulting from FGF19/15 deficiency. We used biochemical
46 quantification and *in vivo* ^{19}F -MRI imaging to compare the accumulation of two previously
47 characterized ^{19}F -bile acid analogue probes, trifluoroacetyl L-lysine and trifluoro-N-methyl-
48 acetamide conjugates of the native human primary bile acid cholic acid (i.e. CA-lys-TFA and
49 CA-sar-TFMA), in gallbladders from WT and FGF15-deficient mice.
50
51
52
53
54
55
56
57
58
59
60

EXPERIMENTAL SECTION

Materials

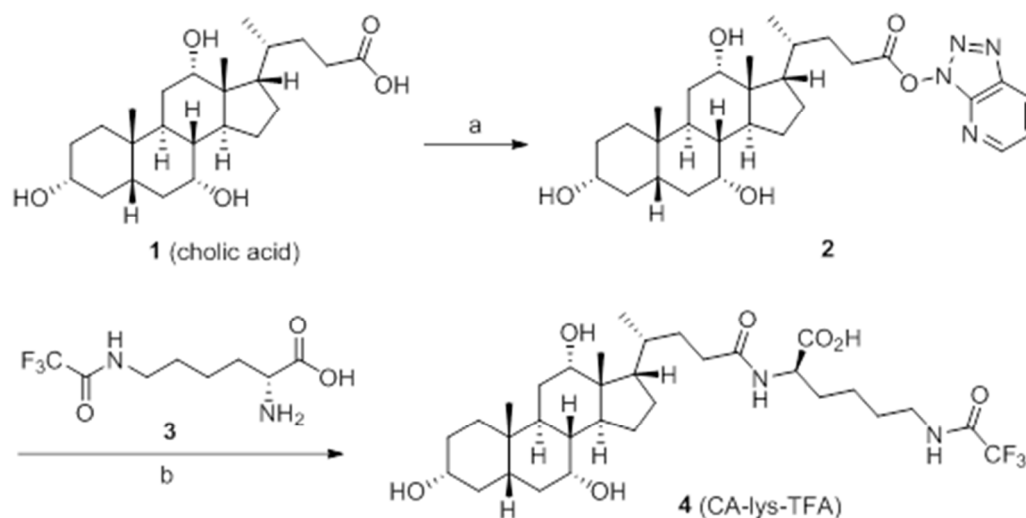
Cholic acid, Dulbecco's phosphate-buffered saline (DPBS), and poly(ethylene glycol) (PEG) 400 were purchased from Sigma Aldrich (St. Louis, Missouri). Compounds **1**, **3**, and **5** were commercially available. We obtained all chemicals from commercial suppliers and used them without further purification.

Synthesis of CA-lys-TFA (Compound 4)

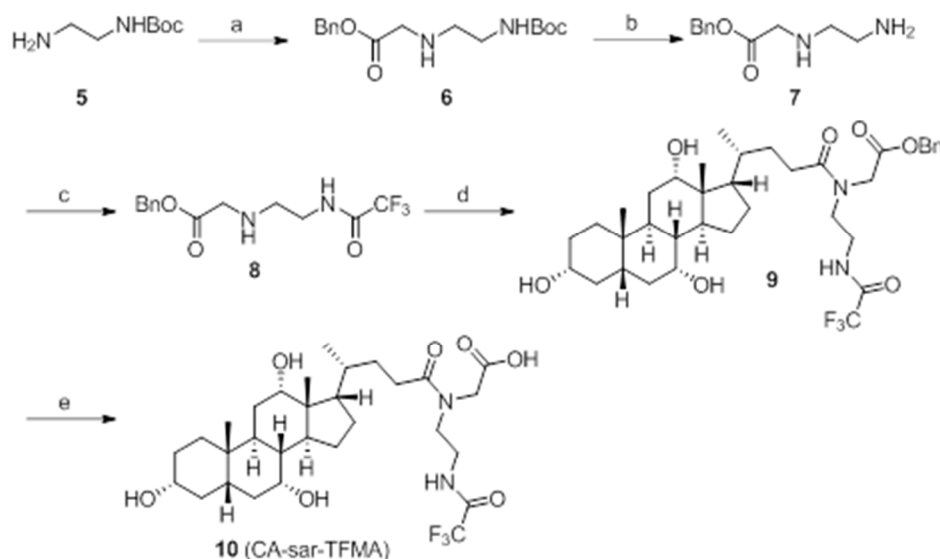
We synthesized CA-lys-TFA, as well as CA-sar-TFMA (below), using an approach modified from that described previously (Supporting Information Synthesis of CA-lys-TFA and CA-sar-TFMA).^{2,4} Briefly, we synthesized target compound **4** as depicted in Figure 1. Activation of cholic acid **1** using HATU yielded the intermediate ester **2**. Coupling of compound **2** with trifluoroacetyl L-lysine **3** provided the final product **4**, CA-lys-TFA, in good yield.

Synthesis of CA-sar-TFMA (Compound 10)

The synthesis of compound **10** began with N-Boc-ethylenediamine **5** (Figure 2). Compound **5** was allowed to react with benzyl bromoacetate to yield compound **6** in high yield. Next, we removed the Boc-protecting group of compound **6** using TFA to generate amine **7**, which was treated with trifluoroacetic anhydride (TFAA) to give compound **8** in high yield. Compound **8** was coupled to compound **2** to obtain the benzyl ester **9** in high yield. Finally, the benzyl-protecting group was removed by catalytic hydrogenation to yield product **10**, CA-sar-TFMA, in good yield.



20 **Figure 1.** Synthesis of Compound 4 (CA-lys-TFA). Reagents and conditions: (a) HATU, Et₃N,
21 DMF, RT, 4 h; (b) DMF, RT, 12 h, 80% for two steps.



42 **Figure 2.** Synthesis of Compound 10 (CA-sar-TFMA). Reagents and conditions: (a) benzyl
43 bromoacetate, NaOH, DMF, RT, 12 h, 78%; (b) TFA, DCM, RT, 1 h; (c) trifluoroacetic
44 anhydride, DCM, RT, 12 h, 83% for two steps; (d) 2, DMF, RT, 12 h; (e) Pd/C, H₂, EtOH, RT,
45 12 h, 81% for two steps.

Chemical Analysis

We visualized analytical thin layer chromatography by ultraviolet light at 254 nm. We recorded ^1H NMR and ^{19}F NMR spectra on a Varian (400 MHz) spectrometer. Mass spectra were recorded using electrospray as the ionization technique. Per NMR, the purity of the final products **4** and **10** were > 95% (Supporting Information Figures S1-S8).

Animals

All animal studies were approved by the Institutional Animal Care and Use Committee of the University of Maryland School of Medicine and the Research and Development Committee at the VA Maryland Health Care System. We conducted animal studies in accordance with the Guide for the Care and Use of Laboratory Animals prepared by the U.S. National Academy of Sciences. Male FGF15-deficient and WT mice (on the same 25% C57BL/6J; 75% 129SvJ mixed genetic background) were kindly provided by Dr. Grace Guo (Rutgers University, Ernest Mario School of Pharmacy, Piscataway, NJ).¹⁰ We housed mice with free access to water and standard mouse chow in a pathogen-free environment with a 12:12-h light/dark cycle for 1 week prior to experiments. After a fast of at least 6 h, mice underwent oral gavage with CA-sar-TFMA and/or CA-lys-TFA in vehicle [60% PEG 400 and 40% DPBS, 8.33 μL per g mouse body weight] and subsequently anesthetized with ketamine/xylazine at different time points. Doses of imaging agents reflect their slight difference in molecular weight and provide the same molar dose in micromole/kg mouse body weight (1.24 mmol/kg for 75 mg/kg CA-sar-TFMA and 78.5 mg/kg CA-lys-TFA; 2.48 mmol/kg for 150 mg/kg CA-lys-TFA).

Oral Disposition Characterization

We characterized the oral disposition of the two bile acid analogues via destructive sampling in *Fgf15*^{-/-} and WT mice through a series of experiments. In a pilot study, four *Fgf15*^{-/-} and four WT mice were concomitantly gavaged with 75 mg/kg CA-sar-TFMA and 78.5 mg/kg CA-lys-TFA. At 7, 10, 24, and 72 h post dosing, we euthanized mice and harvested the gallbladder, liver, and blood. We collected blood into heparinized tubes that we then centrifuged at 12,000g for 10 min. We analyzed supernatants using LC-MS/MS. The liver and gallbladder

1
2
3 were homogenized on ice with a glass tissue homogenizer (Duall size-21; Kimble Chase Life
4 Science, Vineland, New Jersey). We extracted CA-sar-TFMA and CA-lys-TFA with 75% ACN
5 in water (800 μ L for liver and 300 μ L for gallbladder). We centrifuged extracts at 12,000g for 10
6 min before analysis by LC/MS/MS.
7
8
9

10 Favorable gallbladder results from the pilot study led to pharmacokinetic study 1,
11 wherein five *Fgf15*^{-/-} and five WT mice were concomitantly gavaged with 7.5 mg/kg CA-sar-
12 TFMA and 7.85 mg/kg CA-lys-TFA. At 7, 8.5, 10, 16, and 24 h post gavage, we euthanized
13 mice and harvested and processed gallbladders as above. In pharmacokinetic study 2, nine
14 *Fgf15*^{-/-} and nine wild-type mice were concomitantly gavaged with 7.5, 22.5, or 75 mg/kg CA-
15 sar-TFMA and 7.85, 23.5, or 78.5 mg/kg CA-lys-TFA, respectively. We euthanized mice 8.5 h
16 post gavage, and harvested and processed gallbladders as above. In pharmacokinetic study 3,
17 nine *Fgf15*^{-/-} and nine WT mice were concomitantly gavaged in triplicate with 75 mg/kg CA-sar-
18 TFMA and 78.5 mg/kg CA-lys-TFA. We euthanized mice at 7, 8.5, and 10 h post dosing and
19 harvested the gallbladder, small intestine, cut into three equal segments, cecum, and colon. We
20 extracted CA-sar-TFMA and CA-lys-TFA with 75% ACN in water (300 μ L for gallbladder, 450
21 μ L for small intestine segments, 650 μ L for cecum, and 600 μ L for colon). We centrifuged
22 extracts at 12,000g for 10 min before LC-MS/MS analysis.
23
24
25
26
27
28
29
30
31
32
33
34
35

36 ***In Vitro Stability of CA-lys-TFA and CA-sar-TFMA in Mouse Stool***

37
38 We evaluated the ability of mouse stool to hydrolyze CA-lys-TFA and CA-sar-TFMA *in*
39 *vitro*. We collected and pooled stool pellets from multiple *Fgf15*^{-/-} and WT mice maintained in
40 metabolic cages to prevent coprophagia. We removed debris and then lyophilized stool for 2 h
41 using a Thermo Scientific Savant SpeedVac concentrator (Thermo Fisher Scientific, Waltham,
42 MA). Then, we ground stool into a fine powder using a mortar and pestle. We incubated 50-mg
43 aliquots of stool with CA-sar-TFMA or CA-lys-TFA in a water bath maintained at 37°C for 0, 2,
44 4, 8, and 24 h. We quenched samples with ACN, centrifuged at 10,000g for 10 min, and stored
45 them at -80°C until analysis by LC-MS/MS.
46
47
48
49
50
51
52
53
54
55
56
57
58
59
60

In Vitro Stability of CA-sar-TFMA and CA-lys-TFA in Gallbladder Homogenate

To prepare gallbladder homogenates, we collected, pooled, and homogenized in DPBS the gallbladders of four WT mice that had not been gavaged with probes. Aliquots of gallbladder homogenate were prepared in triplicate with CA-sar-TFMA and CA-lys-TFA and incubated in a water bath maintained at 37°C for 0, 20, 40, 60, 90, 120, 240, 480, and 1440 min. Samples were quenched with ACN, centrifuged at 12,000g for 10 min, and stored at -80°C until analysis by LC-MS/MS.

Murine Gallbladder Imaging

After fasting and gavage as described above, we anesthetized mice with ketamine/xylazine injected through an intraperitoneal (i.p.) catheter and imaged them by ¹H MRI and ¹⁹F MRI ~8.5 h after CA-lys-TFA dosing (1.5 h total ¹⁹F acquisition time). Approximately every 30 min throughout imaging, we infused maintenance doses of ketamine/xylazine through the i.p. catheter. The mice remained in the MRI machine for 2 h, for system calibration and ¹H and ¹⁹F MRI acquisition time. On each occasion, we imaged a 30-mM phantom of CA-lys-TFA dissolved in methanol in a short glass NMR tube (5-mm diameter) alongside mice.

Magnetic Resonance Imaging

All *in vivo* MRI data were acquired using identical parameters, as described previously³ (i.e., phantom and animal experiments used identical ¹⁹F and ¹H parameters). Briefly, we performed MRI experiments using a Bruker BioSpec 70/30USR Avance III 7T horizontal bore MR scanner (Bruker Biospin MRI GmbH, Ettlingen, Germany) with a BGA12S gradient system and used Bruker ParaVision 5.1 software for acquisition and processing. The coil was a Bruker 40-mm ¹⁹F/¹H dual-tuned linear volume coil that transmitted and received radiofrequency signals at 300.28 MHz for ¹H and 282.55 MHz for ¹⁹F nuclei. Multislice ¹H MR images used an acquisition time of 6 min and 10 s using a RARE (rapid acquisition with relaxation enhancement) sequence in the cross view of the phantom or animal body. ¹H MRI employed repetition time 1850 ms, RARE factor 8, field of view 4 × 4 cm², echo time 8.58 ms, slice thickness 1.0 mm, matrix size 200 x 200, number of averages 8, and in-plane resolution 200 x

1
2
3 200 μm^2 with 20 slices. ^{19}F images were acquired with a FLASH (fast low angle shot) sequence
4 in an identical region to ^1H MRI. ^{19}F acquisition time was 1 h and 30 min. Parameters were the
5 same as ^1H MRI, but with repetition time 220 ms, echo time 3.078 ms, in-plane resolution $1.25 \times$
6 1.25 mm^2 , matrix size 32×32 , slice thickness 4.0 mm, number of averages 768, and flip angle =
7 30° . We optimized the flip angle using the T1 relaxation time of the phantom. The phantom was
8 a 5-mm diameter shortened glass NMR tube containing 30 mM CA-lys-TFA dissolved in
9 methanol.

10
11 We calculated CA-lys-TFA concentrations in the mouse gallbladder by comparing the
12 mean signal intensity in the region of interest (ROI) identified in the gallbladder to the mean
13 signal intensity in the phantom ROI imaged next to the mouse body. In each case, we drew the
14 ROI to exclude the edges of the phantom and gallbladder, so that signal intensity calculation did
15 not suffer from a partial volume edge effect due to the image resolution. Mean signal intensity
16 was calculated with Bruker ParaVision 5.1. The limit of quantification of ^{19}F signal for this
17 method was previously determined to be 6.82 mM, which corresponds to the noise magnitude of
18 an ROI on the image periphery plus 2.5-times its standard deviation.³ Using this method, there is
19 greater than 99% confidence that voxels with concentrations above this limit represent real ^{19}F
20 signal, and not noise.¹¹

21
22 We used Medical Image Processing, Analysis and Visualization software (MIPAV
23 v7.0.1; CIT, NIH, Bethesda, Maryland) to generate a color ^{19}F MR image of the mice and
24 adjacent phantom. The image threshold used was 0.7 on a scale where the strongest signal (in
25 red) was 1.0.

26 27 28 ***LC-MS/MS Analysis***

29
30 We determined concentrations of CA-sar-TFMA, CA-lys-TFA, and cholic acid by
31 LC/MS/MS using a Waters Acquity UPLC system with triple quadrupole detector (Waters
32 Corporation, Milford, Massachusetts, USA). We used a Waters Acquity UPLC ethylene bridged
33 hybrid C8 $1.7 \mu\text{m}$ $2.1 \times 50 \text{ mm}$ column with a flow rate of 0.4 mL/min. The gradient was as
34 follows (expressed as % ACN in water, all mobile phases include 0.1% formic acid): 50% from 0
35 to 0.5 min, then increased to 95% until 3 min, then decreased to 50% at 3.01 min and held at
36

1
2
3 50% until 4 min. Injection volume was 10 μ L. For CA-lys-TFA, cone voltage was 65 V, dwell
4 time 0.100 s and collision energy 43 V. We used negative electrospray ionization with a multiple
5 reaction monitoring method for the transition 631.15 to 240.92 Da. The method was linear over a
6 range of 5 to 2000 nM ($r^2 \geq 0.97$). For CA-sar-TFMA, cone voltage was 65 V, dwell time 0.100 s
7 and collision energy 36 V. We used negative electrospray ionization with a multiple reaction
8 monitoring method for the transition 603.53 to 213.12 Da. The method was linear over a range of
9 5 to 2000 nM ($r^2 \geq 0.99$). For cholic acid, cone voltage was 66 V, dwell time 0.025 s and
10 collision energy 5 V. We used negative electrospray ionization with a single reaction monitoring
11 method at 407.50 Da. The method was linear over a range of 0.5 to 10000 μ M ($r^2 \geq 0.96$).
12
13
14
15
16
17
18
19
20

21 *Statistical Analysis*

22
23
24 Error shown in the text and figures is standard error of the mean. We used Student's
25 paired *t*-test to evaluate stability data. We used Student's unpaired *t*-test to evaluate
26 concentration differences of CA-sar-TFMA and CA-lys-TFA in FGF15-deficient versus WT
27 mouse. We considered a *p* value ≤ 0.05 significant.
28
29
30
31
32
33
34
35
36
37
38
39
40
41
42
43
44
45
46
47
48
49
50
51
52
53
54
55
56
57
58
59
60

RESULTS

Oral Disposition Characterization

We calculated the concentrations of CA-lys-TFA and CA-sar-TFMA in the gallbladder and liver by assuming an organ density of 1 g/mL. Gallbladder concentrations of ^{19}F at 10 h were above the ^{19}F MRI limit of detection, as previously defined, and liver and plasma concentrations were below the limit of detection.³ The gavage concentration of 75 mg/kg CA-sar-TFMA and 78.5 mg/kg CA-lys-TFA showed high accumulation in the WT mouse gallbladder at 10 h after oral dosing with a >20 fold difference compared to the gallbladder of the FGF15-deficient mouse (Figure 3). In contrast, CA-sar-TFMA and CA-lys-TFA concentrations in the liver and plasma were at least 1000-fold lower on average than in the gallbladder; note the μM scales for liver and plasma vs mM scale for gallbladder. The dose-response curves showed a linear relationship for both CA-lys-TFA and CA-sar-TFMA (Figure 4).

Given the results from the pilot study, 8.5 h was included as an additional time point to better elucidate the peak concentration. Peak concentration occurred in gallbladders of mice at 8.5 h for both compounds at the higher gavage concentration of 75 mg/kg CA-sar-TFMA and 78.5 mg/kg CA-lys-TFA when tested in triplicate (Figure 5A-B). Differences at the 8.5-h time point were statistically significant and showed a >2 fold difference when comparing WT to *Fgf15*^{-/-} mice ($p = 0.04$ and $p = 0.03$, CA-sar-TFMA and CA-lys-TFA, respectively). Gallbladder concentrations in WT mice at 8.5 h were above the ^{19}F MRI limit of detection, whereas all concentrations in the small intestines, cecum, and colon were below the limit of detection (Figure 5C-G). Concentrations of CA-sar-TFMA and CA-lys-TFA between WT and *Fgf15*^{-/-} mice in the small intestines, cecum, and colon were not statistically different.

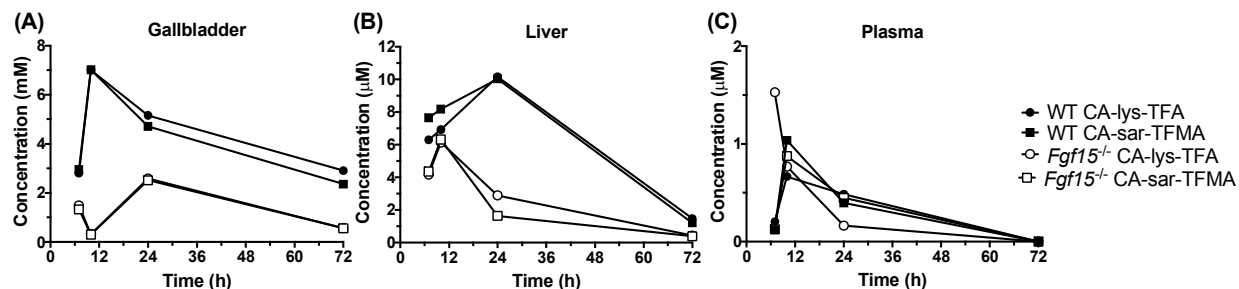


Figure 3. Concentration versus time for CA-lys-TFA (circles) and CA-sar-TFMA (squares) in the gallbladder (A), liver (B), and plasma (C) harvested from WT (closed symbols) and FGF15-deficient (open symbols) mice after concomitant oral administration of 75 mg/kg CA-sar-TFMA and 78.5 mg/kg CA-lys-TFA. ¹⁹F-labeled bile acid analogues were simultaneously co-administered to the same animal. Gavage with the two ¹⁹F-labeled bile acid analogues resulted in much higher concentrations in the gallbladder than the liver or plasma. In gallbladder and liver, bile acid analogue exposure was greater in WT mice than FGF15-deficient mice. Each data point reflects n = 1 mouse from destructive sampling.

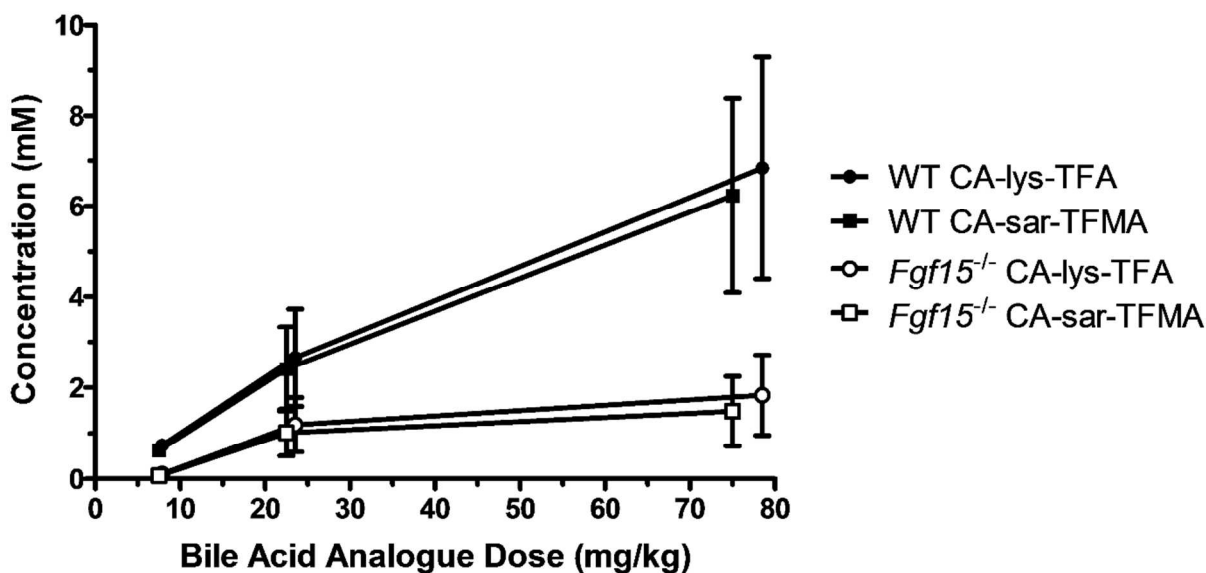


Figure 4. Dose-response curve in the gallbladder of WT (closed) and FGF15-deficient (open symbols) mice after concomitant oral administration of CA-lys-TFA (circles) and CA-sar-TFMA (squares). Larger doses resulted in higher gallbladder concentrations of ¹⁹F-labeled bile acid analogues. Each data point reflects n = 3 mice.

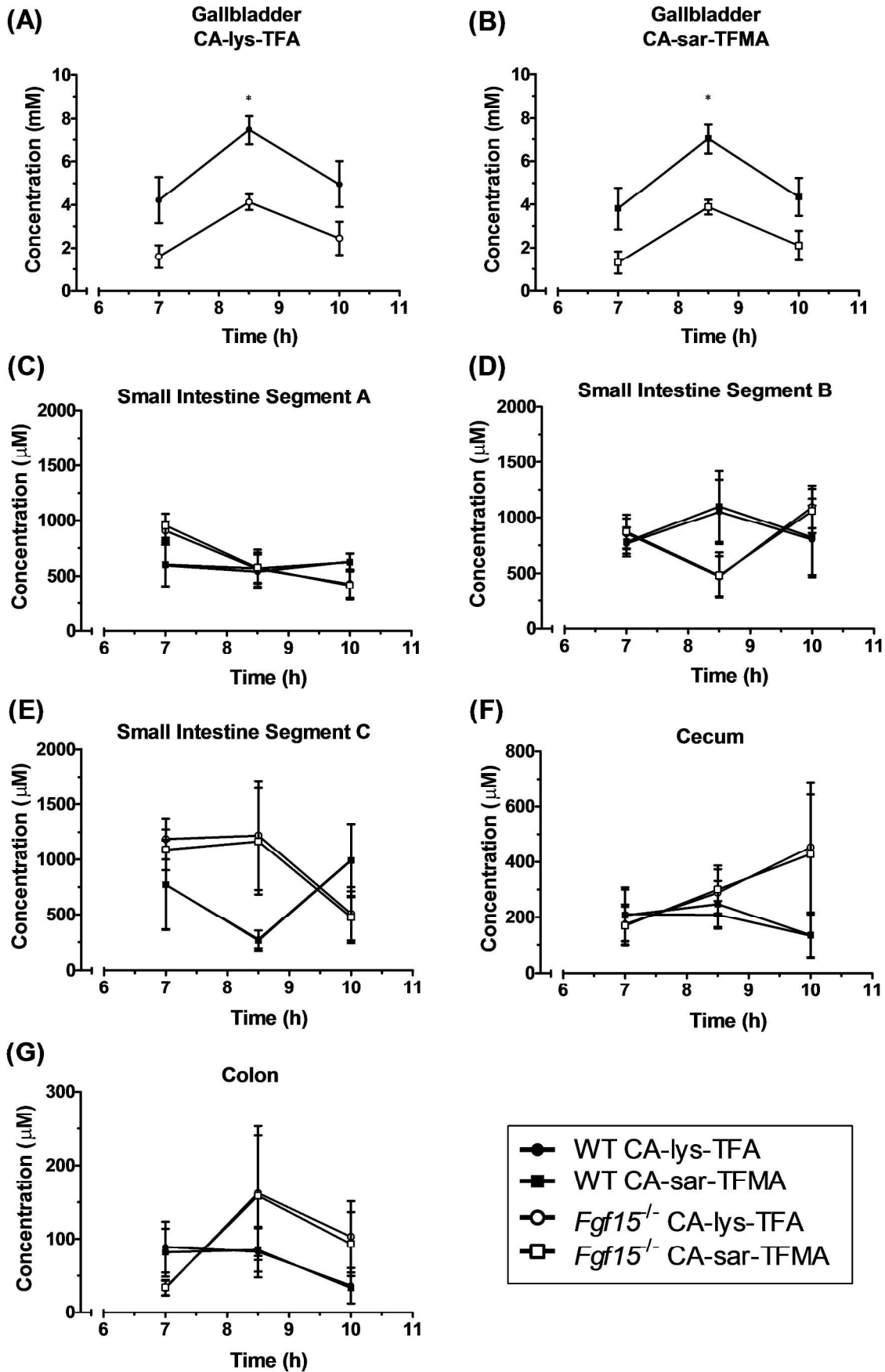


Figure 5. Concentration versus time of CA-lys-TFA (circles) and CA-sar-TFMA (squares) in the gallbladder (A, B), small intestine (C, D, E), cecum (F), and colon (G) of WT (closed symbols) and FGF15-deficient (open symbols) mice after concomitant oral administration of 75 mg/kg CA-sar-TFMA and 78.5 mg/kg CA-lys-TFA. All panels use the same symbols. The only statistical difference in ^{19}F -labeled bile acid analogue concentration between FGF15-deficient and WT mice was in the gallbladder at 8.5 h (A, $p = 0.04$ and B, $p = 0.03$). Each data point reflects $n = 3$ mice.

In Vitro Stability of CA-sar-TFMA and CA-lys-TFA in Mouse Stool

Incubation of CA-sar-TFMA and CA-lys-TFA in stool showed no significant degradation at the longest time tested ($p > 0.05$, Figure 6).

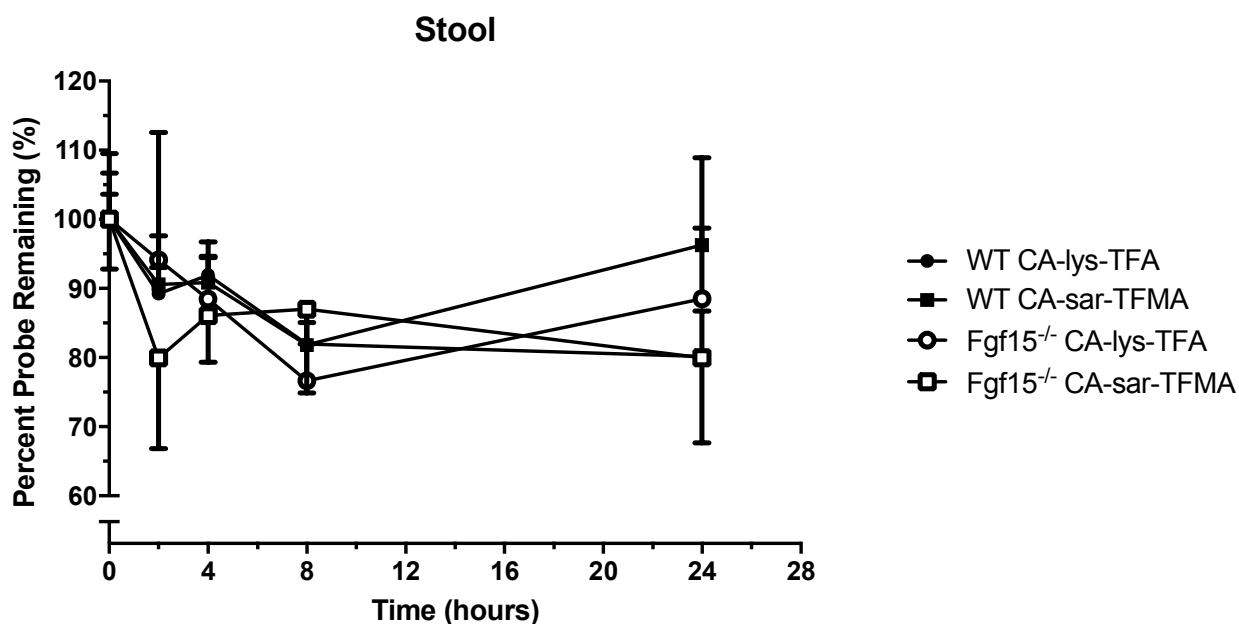


Figure 6. Percent remaining versus time of CA-lys-TFA (circles) and CA-sar-TFMA (squares) in stool samples of WT (closed symbols) and FGF15-deficient (open symbols) mice performed in triplicate. Each ^{19}F -labeled bile acid analogue exhibited favorable stability over 24 h in stool. There was about a 15% loss of each ^{19}F -labeled bile acid analogue over 24 h.

In Vitro Stability of CA-sar-TFMA and CA-lys-TFA in Gallbladder Homogenate

Incubation of CA-sar-TFMA and CA-lys-TFA in gallbladder homogenates showed statistically significant degradation at the longest duration tested ($p < 0.01$). Cholic acid also showed statistically significant degradation ($p < 0.01$). However, degradation of CA-sar-TFMA and CA-lys-TFA was slightly more than that of cholic acid, which exhibited about a 12% loss at

the longest duration tested (Figure 7).

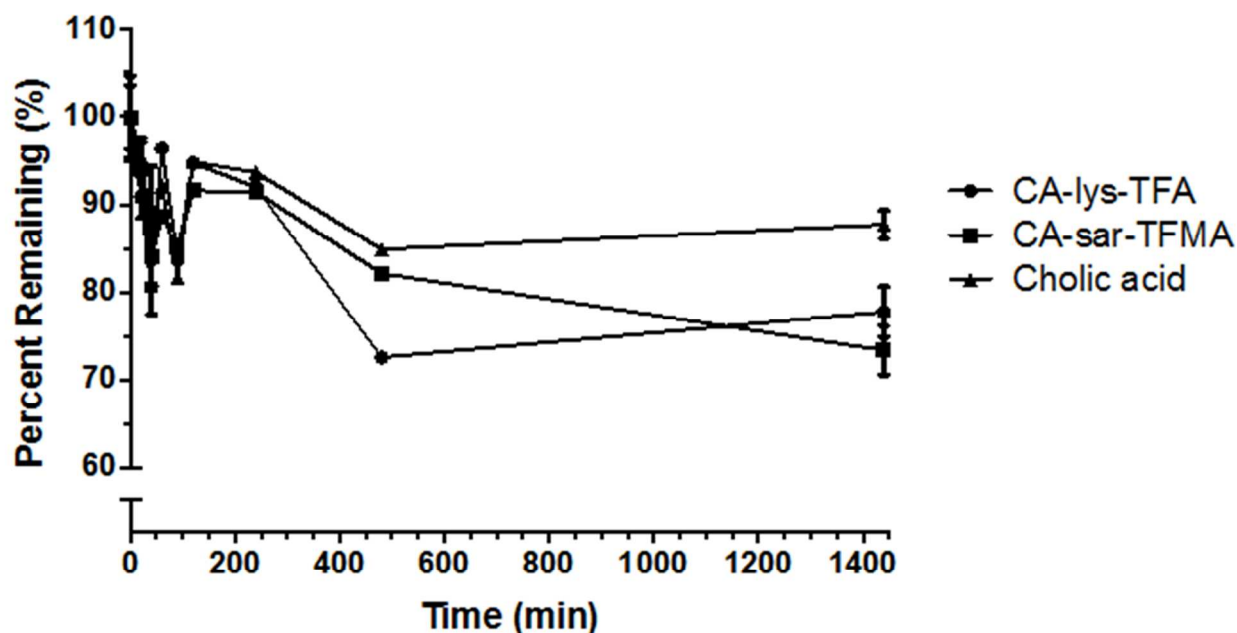


Figure 7. Percent remaining versus time of CA-lys-TFA (circles), CA-sar-TFMA (squares), and cholic acid (triangles) in pooled gallbladder homogenate prepared in triplicate from four WT mice. The two ^{19}F -labeled bile acid analogues exhibited favorable stability over 24 h in WT gallbladder homogenate. There was about a 25% decrease in each bile acid analogue over 24 h. For reference, there was a 12% loss of cholic acid over 24 h.

Murine Gallbladder Imaging

Based on LC-MS/MS results of the peak accumulation occurring at 8.5 h, mice underwent MRI at 8.5 h after oral gavage of 150 mg/kg CA-lys-TFA – we imaged mice once followed by euthanasia. We visualized strong ^{19}F MRI signals emanating from the gallbladders of all WT mice tested (Figure 8A). Overlay of images obtained by ^1H and ^{19}F MRI signal acquisition confirmed ^{19}F signals emanated from the gallbladder (Figure 8A). CA-lys-TFA concentration in the gallbladder, calculated by normalizing the average intensity of the gallbladder ROI to that within the phantom, was determined to be 27 mM.

As predicted from our LC-MS/MS data, MRI of three consecutive *Fgf15*^{-/-} mice revealed no detectable signal (Figure 8B); as a control, we observed a robust ^{19}F MRI signal emanating

from phantoms placed next to these mice.

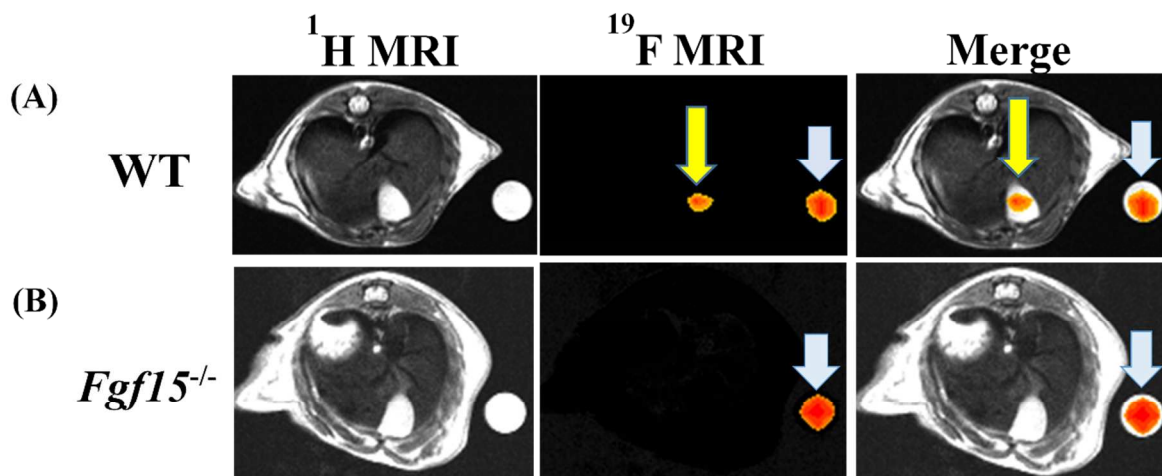


Figure 8. ^{19}F MRI in WT and FGF15-deficient mice gavaged with 150 mg/kg CA-lys-TFA. We detected a ^{19}F signal only in gallbladders from WT mice. Arrowheads (blue) and arrows (yellow) indicate ^{19}F signals emanating from phantoms and gallbladder, respectively. This imaging result, representative of findings in three separate WT and FGF15-deficient mice, is consistent with the LC/MS/MS-based observations.

DISCUSSION

Performance of Bile Acid Analogues

To address the unmet need for a safe and accurate method of diagnosing bile acid diarrhea due to FGF19 deficiency in countries like the United State where clinicians do not have access to SeHCAT testing, we evaluated a novel noninvasive approach using *in vivo* ^{19}F MRI. We tested the ability of gavage with a ^{19}F -bile acid analogue, CA-lys-TFA, to detect abnormal bile acid transport in FGF15-deficient mice, an animal model of human FGF19 deficiency. We, and others, have shown that, like humans with FGF19 deficiency, FGF15-deficient mice have increased fecal bile acid excretion.¹²⁻¹⁵ We detected low quantities of intact CA-lys-TFA and CA-sar-TFMA in the stool, with more in stool from FGF15-deficient mice than from wild-type mice (Supporting Information Figure S9).

1
2
3 In the present communication, our LC-MS/MS data show that, in both WT and *Fgf15*^{-/-}
4 mice, each ¹⁹F-bile acid analogue accumulated in the gallbladder and, at much lower
5 concentrations, in the liver, plasma, small intestine, and colon (Figures 3 and 5). Notably, across
6 three doses, we observed that FGF15 deficiency reduced the concentrations of ¹⁹F-labeled bile
7 acid analogues in gallbladder bile (Figure 4). In WT mice, average gallbladder bile CA-lys-TFA
8 and CA-sar-TFMA concentrations exceeded our ¹⁹F MRI limit of detection (i.e. above 2.27 mM,
9 as there are three equivalent fluorine atoms in each structure).³ In contrast, the concentrations of
10 these molecules measured by LC-MS/MS in tissues from FGF15-deficient mice were generally
11 below the ¹⁹F MRI limit of detection (Figures 3 - 5). The lack of ¹⁹F MRI signals from
12 gallbladders of FGF15-deficient mice 8.5 h after gavage with 150 mg/kg CA-lys-TFA
13 substantiated this finding; gallbladders of comparably treated WT mice provided strong imaging
14 signals (see representative examples in Figure 8).
15
16
17
18
19
20
21
22
23

24 Interestingly, CA-lys-TFA and CA-sar-TFMA provided similar *in vivo* pharmacokinetic
25 distribution profiles, although prior *in vitro* studies suggested greater stability against
26 cholyglycine hydrolase for CA-sar-TFMA compared to CA-lys-TFA.^{2,4} To address the similar
27 *in vivo* stabilities of CA-lys-TFA and CA-sar-TFMA observed here, we assessed the stability of
28 these molecules in murine stool and gallbladder homogenates. Our finding of similar stability of
29 CA-lys-TFA and CA-sar-TFMA in stool (Figure 6) and gallbladder homogenates (Figure 7) is
30 consistent with the compounds' similar *in vivo* stability. In mice, cholyglycine hydrolase does
31 not appear to be a large determinant of CA-sar-TFMA or CA-lys-TFA stability *in vivo*. Overall,
32 neither CA-sar-TFMA nor CA-lys-TFA is preferred over the other. These observations highlight
33 the importance of confirming *in vitro* observations using *in vivo* models.
34
35
36
37
38
39
40
41
42
43

44 **Potential Use of Fluorinated Bile Acid Analogues**

45
46 Previously, we synthesized CA-lys-TFA and CA-sar-TFMA and evaluated the *in vitro*
47 stability and affinity of these molecules for ASBT and Na⁺/taurocholate co-transporting
48 polypeptide (NTCP, *SLC10A1*).^{2,4} In addition, to assess their ability to concentrate in the
49 gallbladder, the ¹⁹F-bile acid analogues' ¹⁹F MRI signals were measured in the gallbladders of
50 WT and ASBT-deficient mice *in vivo*.²⁻⁴ In the present study, we evaluated CA-lys-TFA and
51 CA-sar-TFMA in FGF15-deficient mice.
52
53
54
55
56
57
58
59
60

1
2
3 In humans, reduced levels of FGF19 impair bile acid homeostasis within the
4 enterohepatic circulation. Specifically, the liver continues to synthesize bile acids despite the
5 presence of abundant bile acids in the terminal ileum. The loss of feedback repression of bile
6 acid synthesis by FGF19 results in excess spillage of bile acids into the colon that simulates
7 electrolyte and water secretion, inflammation, and motility, thus leading to diarrhea. Bile acid
8 uptake from the distal small intestine by ASBT is unimpaired, but the excess bile acids in the
9 ileum overwhelm ASBT transport capacity, causing diarrhea.¹⁶ Approximately one of three
10 individuals diagnosed with IBS-D may actually have bile acid diarrhea.⁵ Distinguishing these
11 conditions is important; incorrectly attributing bile acid diarrhea to IBS may result in prolonged
12 treatment with costly, ineffective drugs that may have substantial side effects. The resulting
13 therapeutic failure may have a negative impact on the quality of life.

14
15
16
17
18
19
20
21
22
23 Conceptually, the clinical use of ¹⁹F bile acid analogue-MRI to diagnose bile acid
24 diarrhea is attractive; the test would not require phlebotomy or exposure to ionizing radiation.
25 Nonetheless, there are limitations to our work and to the translational potential of this test. We
26 employed FGF15-deficient mice, which excrete excess bile acids, but do not exhibit diarrhea.^{12,15}
27 Thus, although these mice mimic the physiology of FGF19 deficiency, the clinical phenotype is
28 different; this difference may reflect differences between murine and human colon physiology,
29 diet, and other factors. Additionally, we needed high doses to detect analogues in mouse
30 gallbladder via MRI, employing a 1.5-h acquisition time. The necessary dose and acquisition
31 time for use in humans would require clinical testing. Since ¹⁹F bile acid analogue-MRI requires
32 the presence of a functional gallbladder, this test would not work in experimental animals
33 lacking a gallbladder (e.g. rats) or in humans after cholecystectomy. Finally, a major obstacle to
34 such a diagnostic approach is the current paucity of clinical MRI facilities equipped with the
35 appropriate hardware (coil) and software needed to detect fluorine signals.

36
37
38
39
40
41
42
43
44
45
46 Overall, our findings support the concept that increased fecal bile acids in FGF15/19
47 deficiency result from a reduction in the fraction of intestinal bile acids transported by ASBT.
48 Moreover, ¹⁹F-bile acid MRI shows potential as a novel test for diagnosing bile acid diarrhea
49 resulting from FGF19 deficiency. Nonetheless, we must address and overcome several
50 limitations and obstacles before ¹⁹F-bile acid MRI can transition to clinical practice.
51
52
53
54
55
56
57
58
59
60

SUPPORTING INFORMATION

Synthesis of CA-lys-TFA and CA-sar-TFMA, ¹H-NMR of compound **4**, ¹⁹F-NMR of compound **4**, HRMS of compound **4**, ¹H-NMR of compound **6**, ¹H-NMR of compound **8**, ¹H-NMR of compound **10**, ¹⁹F-NMR of compound **10**, HRMS of compound **10**, and mass of CA-lys-TFA and CA-sar-TFMA in stool samples per 24-h stool collection

ACKNOWLEDGEMENTS

We thank Dr. Grace Guo, Ernest Mario School of Pharmacy, Rutgers University, for providing FGF15-deficient and WT control mice. We also thank Drs. Alan F. Hofmann, Paul A. Dawson, and Michael Camilleri for their helpful discussions and guidance. This work was supported by Food and Drug Administration [U01FD005946], National Institutes of Health, National Institute of Diabetes and Digestive and Kidney Diseases [Grants R21 DK093406 and T32 DK067872], and a Merit Review Award [Grant BX002129] from the United States Department of Veterans Affairs Biomedical Laboratory Research and Development Program. The contents do not represent the views of the U.S. Department of Veterans Affairs or the United States Government.

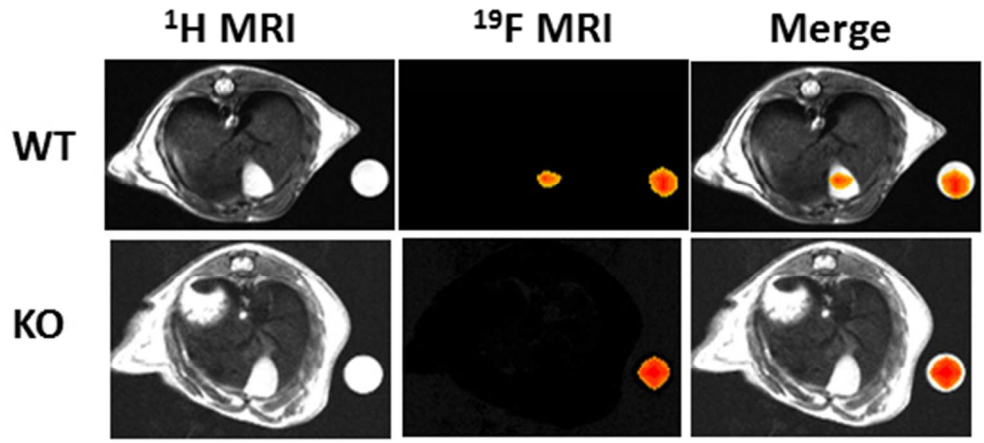
ABBREVIATIONS USED

ASBT, the apical sodium dependent bile acid transporter; C4, 7 α -hydroxy-4-cholestene-3-one; CA, cholic acid; DPBS, Dulbecco's phosphate buffered saline; EtOAc, ethyl acetate; FGF/Fgf, fibroblast growth factor; FLASH, fast low angle shot; IBS-D, diarrhea predominant-irritable bowel syndrome; IP, intraperitoneal; LC-MS/MS, liquid chromatography/ tandem mass spectrometry; MRI, magnetic resonance imaging; NTCP, the Na⁺/taurocholate co-transporting polypeptide; PEG, polyethylene glycol; RARE, rapid acquisition with relaxation enhancement; rf, radio frequency; ROI, region of interest; SeHCAT, ⁷⁵Selenium homotaurocholic acid retention test; TFAA, trifluoroacetic anhydride; WT, wild type

REFERENCES

- (1) Dawson P. A. Bile formation and the enterohepatic circulation. In: Johnson L. R., ed. *Physiology of the Gastrointestinal Tract*. Oxford: Academic Press; 2012:1461-84.
- (2) Vivian D., Cheng K., Khurana S., Xu S., Kriel E. H., Dawson P. A., Raufman J. P., Polli J. E. In vivo performance of a novel fluorinated magnetic resonance imaging agent for functional analysis of bile acid transport. *Mol Pharm* **2014**;11:1575-82.
- (3) Vivian D., Cheng K., Khurana S., Xu S., Dawson P. A., Raufman J. P., Polli J. E. Design and evaluation of a novel trifluorinated imaging agent for assessment of bile acid transport using fluorine magnetic resonance imaging. *J Pharm Sci* **2014**;103:3782-92.
- (4) Vivian D., Cheng K., Khurana S., Xu S., Whiterock V., Witter D., Lentz K. A., Santone K. S., Raufman J. P., Polli J. E. Design and characterization of a novel fluorinated magnetic resonance imaging agent for functional analysis of bile Acid transporter activity. *Pharm Res* **2013**;30:1240-51.
- (5) Pattni S., Walters J. R. F. Recent advances in the understanding of bile acid malabsorption. *Br Med Bull* **2009**;92:79-93.
- (6) Wedlake L., & Andreyev, J. *Textbook of Clinical Gastroenterology and Hepatology*. 2 ed. Oxford, UK: Wiley-Blackwell; 2012.
- (7) Pattni S. S., Brydon W. G., Dew T., Walters J. R. F. Fibroblast Growth Factor 19 and 7 α -Hydroxy-4-Cholesten-3-one in the Diagnosis of Patients With Possible Bile Acid Diarrhea. *Clin Transl Gastroenterol* **2012**;3:e18.
- (8) Westergaard H. Bile Acid malabsorption. *Current treatment options in gastroenterology* **2007**;10:28-33.
- (9) Felton J., Cheng K., Said A., Shang A. C., Xu S., Vivian D., Metry M., Polli J. E., Raufman J.-P. Using Multi-fluorinated Bile Acids and In Vivo Magnetic Resonance Imaging to Measure Bile Acid Transport. *JoVE* **2016**:e54597.
- (10) Kong B., Huang J., Zhu Y., Li G., Williams J., Shen S., Aleksunes L. M., Richardson J. R., Apte U., Rudnick D. A., Guo G. L. Fibroblast growth factor 15 deficiency impairs liver regeneration in mice. *American journal of physiology Gastrointestinal and liver physiology* **2014**;306:G893-902.
- (11) Srinivas M., Morel P. A., Ernst L. A., Laidlaw D. H., Ahrens E. T. Fluorine-19 MRI for visualization and quantification of cell migration in a diabetes model. *Magnetic resonance in medicine* **2007**;58:725-34.

- 1
2
3 (12) Inagaki T., Choi M., Moschetta A., Peng L., Cummins C. L., McDonald J. G., Luo G., Jones
4 S. A., Goodwin B., Richardson J. A., Gerard R. D., Repa J. J., Mangelsdorf D. J., Kliewer S. A.
5 Fibroblast growth factor 15 functions as an enterohepatic signal to regulate bile acid
6 homeostasis. *Cell metabolism* **2005**;2:217-25.
7
8 (13) Walters J. R., Tasleem A. M., Omer O. S., Brydon W. G., Dew T., le Roux C. W. A new
9 mechanism for bile acid diarrhea: defective feedback inhibition of bile acid biosynthesis. *Clinical*
10 *gastroenterology and hepatology : the official clinical practice journal of the American*
11 *Gastroenterological Association* **2009**;7:1189-94.
12
13 (14) Hofmann A. F., Mangelsdorf D. J., Kliewer S. A. Chronic diarrhea due to excessive bile acid
14 synthesis and not defective ileal transport: a new syndrome of defective fibroblast growth factor
15 19 release. *Clinical gastroenterology and hepatology : the official clinical practice journal of the*
16 *American Gastroenterological Association* **2009**;7:1151-4.
17
18 (15) Cheng K., Metry M., Felton J., Shang A. C., Drachenberg C. B., Xu S., Zhan M.,
19 Schumacher J., Guo G. L., Polli J. E., Raufman J.-P. Diminished gallbladder filling, increased
20 fecal bile acids, and promotion of colon epithelial cell proliferation and neoplasia in fibroblast
21 growth factor 15-deficient mice. *Oncotarget* **2018**;9:25572-85.
22
23 (16) Camilleri M. Bile Acid Diarrhea: Prevalence, Pathogenesis, and Therapy. *Gut Liver*
24 **2015**;9:332-9.
25
26
27
28
29
30
31
32
33
34
35
36
37
38
39
40
41
42
43
44
45
46
47
48
49
50
51
52
53
54
55
56
57
58
59
60



22 ¹⁹F MRI was only detected in WT mice and not in FGF15-deficient mice gavaged with CA-lys-TFA.

23
24 139x64mm (96 x 96 DPI)